iPP/HDPE Blends: Interactions at Lower HDPE Contents

H. P. BLOM, J. W. TEH, and A. RUDIN*

Institute for Polymer Research, Department of Chemistry, University of Waterloo, Waterloo, Ontario N2L 3G1, Canada

SYNOPSIS

Mechanical and rheological properties of blends of polypropylene (PP) and linear polyethylene (PE) were studied, with particular attention to the effects of aging of such mixtures. These two olefin polymers are basically incompatible. In PP-rich blends, addition of high-density PE (HDPE) causes only a slight decrease in tensile properties and impact resistance of injection-molded specimens. In all cases, annealed specimens have higher moduli and lower impact strength than as-molded products. While none of these changes are very drastic, the addition of small amounts of HDPE was observed to result in a serious decrease of gate-region impact resistance of thin-walled moldings. Blends with 10–20% HDPE exhibited an unexpected interaction in tensile, thermal, and melt-flow properties as well as in crystallization behavior. © 1995 John Wiley & Sons, Inc.

INTRODUCTION

In recent years increasing attention has been devoted to studying blends of polyolefins, especially polypropylene (PP) and polyethylene (PE). There are a number of reasons for this. On the one hand, these blends are interesting from a theoretical point of view if one considers that these polymers should be miscible based on their solubility parameters, $\delta = 16.8\ (J/cm^3)^{1/2}$ for PP and $\delta = 17.0\ (J/cm^3)^{1/2}$ for PE. However, it is well documented that PP and PE are incompatible and immiscible. On the other hand, increased environmental concerns are resulting in the collection of more and more household waste for recycling purposes. Due to the fact that complete separation of postconsumer PE and PP is at present very costly, and in some cases impossible, it is necessary to develop a sound understanding of these polyolefin blends. It is also important to consider the effect of aging (leading to possible phase separation) on these blends, in light of their immiscibility. Very little attention has been paid to aging phenomena of isotactic PP (iPP)/high-density PE (HDPE) blends in the literature. With these considerations in mind, we set about to investigate iPP/HDPE blends. Our results are presented herein.

EXPERIMENTAL

Materials

The PP used in this study was an injection-molding grade iPP supplied by Shell Canada Limited. It had a melt flow index (MFI) of 20°/min (230°C, 2.16 kg). The molecular weight as determined by size exclusion chromatography[1] was $M_n = 22{,}000$, $M_w = 166{,}000$, and $M_z = 509{,}000$ ($M_w/M_n = 7.6$). The PP had a density of 0.91 g/cm^3. HDPE was supplied by DuPont Canada Inc., and had an MFI of 5°/min (190°C, 2.16 kg). It had a density of 0.96 g/cm^3, and a molecular weight of $M_n = 20{,}000$, $M_w = 66{,}000$, and $M_z = 276{,}000$ ($M_w/M_n = 3.4$). Table I lists the blends studied in this project.

Melt Extrusion Blending

All samples (including the pure homopolymers) were melt blended in a Leistritz LSM corotating intermeshing twin-screw extruder. The barrel temperature profile is shown in Table II. Zones 1–4 comprised the melting and conveying section of the barrel; zones 5–8 were the mixing and shearing sec-

* To whom correspondence should be addressed.

Journal of Applied Polymer Science, Vol. 58, 995–1006 (1995)
 CCC 0021-8995/95/060995-12

Table I Study Blends

PP (wt %)	HDPE (wt %)
100	0
95	5
90	10
85	15
80	20
75	25
0	100

tion and contained kneading and reverse flight elements (to enhance mixing); and zones 9 and 10 were the final transport and metering section. The feed rate was 100 ± 10 g/min, the screw speed was 35 rpm, the die temperature was 190°C, and the die pressure was ~ 17 bar. The barrel length was 1.2 m, and the residence time was approximately 3 min. The barrel was purged between batches with 2 kg of the new blend to remove all traces of the previous blend. The extrudate was frozen in-line in a water bath (~ 10°C), air dried, and granulated.

Mechanical Properties

Impact and Tensile Tests

Impact bars (6.2 × 12.7 × 76 mm^3) and dumbbell tensile test pieces (ASTM D638 Type I) were prepared by injection molding on a Battenfeld BSKM 50-ton press at 190–210°C barrel temperature, 3.22 MPa injection pressure, 40°C mold temperature, and 1.2 s injection time. Impact specimens were notched (30°) to a depth of 2.0 mm the day they were molded. Fresh samples are those that were aged at room temperature for 1–2 weeks. Annealed samples are those that were aged in an oven set at 75°C for 7 days. An instrumented impact tester[2] was used to determine the Charpy notched impact strength. The hammer velocity was 1.0 ± 0.1 m/s. Results presented in this article are averages of 10–14 specimens. Typical output from the impact tester is shown in Figure 1. The top trace is the output from the highly sensitive load cell mounted directly behind the nose of the hammer, and the area under this curve is related to the impact strength. The lower "tooth" trace is the optical response output obtained from a small comb assembly that passed through a laser/photocell detector device. The dimensions of the comb are accurately known, enabling the velocity of the hammer before and after impact to be determined, from which the impact strength could be calculated. The impact strengths reported in this study were calculated from the kinetic energy loss of the hammer.

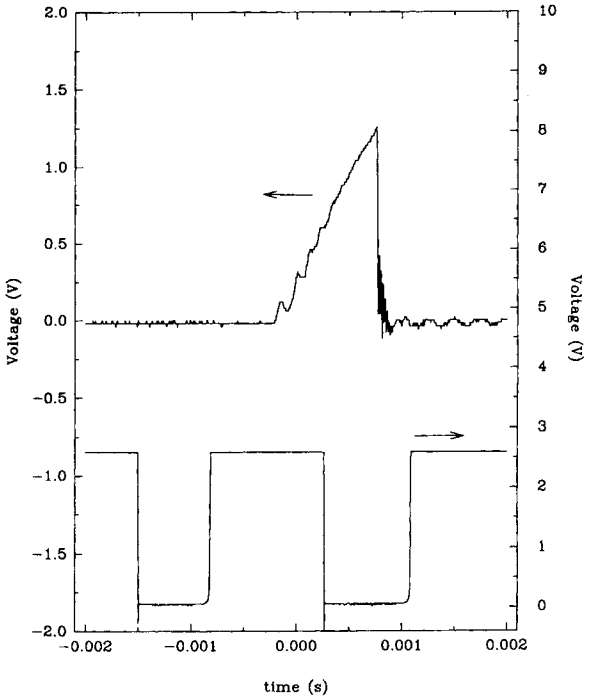

Figure 1 Typical output from the instrumented Charpy impact tester showing the impact event (top trace) and a portion of the "tooth" trace (lower trace).

Tensile tests were performed on an Instron tensile tester at a crosshead speed of 25.4 cm/min and an initial jaw separation of 10 cm. A computer was connected to the Instron load cell, and a data acquisition program read the force recorded by the load cell at a rate of 10 Hz, and plotted the force versus the time. The time and the deformation are related by

Table II Temperature Profile Used in Twin Screw Extruder

Zone	1	2	3	4	5	6	7	8	9	10
Temp:										
Set	20	50	170	180	190	190	190	190	190	190
Actual	68	100	170	180	190	190	190	190	190	190

Temperatures are in degrees Celsius.

the crosshead speed. A relatively high crosshead speed was employed because those blends that contained a high percentage of HDPE experienced cold-drawing at lower crosshead speeds, and stretched beyond the deformation limit of the instrument before failure. Results presented are averages for seven specimens.

Gate Puncture Tests

Thin-walled containers were injection molded on an Engel ES-125 injection molder containing a reciprocating screw and fitted with a thin-walled container mold (635-μm wall thickness). The barrel temperature varied from 230°C at the feed port to 270°C at the nozzle. The average injection velocity was 14.7 cm/min, with an injection pressure of 12.4 MPa. The mold temperature was set at 30°C.

The gate puncture test is an in-house test developed by Shell Canada Limited and is used to determine the gate strength of molded thin-walled containers. A 50-kg load cell, attached to the crosshead of an Instron Model 1122, was fitted with a steel, blunt-nosed dart. The container was positioned upside down in such a way that as the crosshead descended, the dart met the container slightly beside the gate of the molded container. The crosshead speed was set at 1 m/min. A total of 10 containers were tested. Failure occurred either in a brittle mode, with the bottom of the container splitting apart, or in a ductile mode, in which case the base of the container bent. The gate puncture strength, arbitrarily defined as the maximum load, which occurred just prior to failure, was averaged from each of the 10 containers.

DSC Analysis

The melting and crystallization behavior of the blends were studied by differential scanning calorimetry (DSC) using a Perkin Elmer DSC-2. All samples were approximately 10 mg. Each sample was analyzed in the following way:

1. The sample, encapsulated in an aluminum pan, was placed in the DSC sample holder at 67°C. A melting endotherm was recorded as the temperature was ramped from 67° to 180°C at 5°C/min.
2. The sample was left at 180°C for 30 min. A cooling crystallization exotherm was then recorded as the sample temperature was decreased from 180° to 67°C at 1°C/min.
3. The sample was then removed from the DSC and allowed to age at room temperature. Between 24 and 48 h later, the same sample was again placed in the DSC at 67°C. A melting endotherm was recorded as the sample was heated from 67° to 180°C at 5°C/min.

To gauge the reproducibility of our measurements, the DSC test was repeated for three samples of each blend. Any variation in these results is also, by implication, an indication of the homogeneity of the blends.

Thus, we obtained three thermograms from each sample. The first one is a melting endotherm of a quenched sample (i.e., a piece of pellet that had been melt extruded and rapidly cooled in the water bath). The second was a crystallization exotherm of a sample that was completely melted and had been given an opportunity to phase separate. It is conceivable that the quenched sample had some cocrystallized domains, and we assume that prolonged heating at 20°C above the melting point of iPP would destroy all of these regions and allow the PE and iPP phases to separate. The final thermogram was one for a slow-cooled sample. For incompatible crystalline blends, we expect to observe two distinct peaks, one for PE and another for iPP. The first and third thermograms can then be compared to each other, and any differences from cooling histories could be ascertained.

The heat of fusion was calculated based on the area under a given peak and the total weight of the sample using the DSC software. The heats of fusion of the iPP and HDPE were then adjusted with the appropriate weight of iPP and HDPE in the blend to account for the fact that only a percentage of the sample was either iPP or HDPE. This later correction assumed, of course, that the sample had the same composition as the bulk of the blend.

Dynamic Mechanical Analysis

Melt-blended pellets were introduced between the 25-mm-diameter plates of a Rheometrics 605 dynamic mechanical spectrometer, and compression molded into a disk of 2-mm thickness at 180°C. The temperature was varied between 180° and 210°C, in 10°C intervals. The environment was continually purged with nitrogen gas to minimize thermooxidative degradation. Dynamic mechanical properties were obtained at a strain of 30%, and the frequency was varied between 0.03 and 100 rad/s (equivalent to 0.188–625 s^{-1}). The strain of 30% was chosen because the blends exhibited linear behavior at this strain. The zero-shear viscosity was obtained by fit-

ting the viscosity/frequency data to the Ellis model.[3] The activation energy of flow was calculated from plots of the complex viscosity (η^*) versus frequency (ω) at the four temperatures (180°, 190°, 200°, 210°C) using the Rheometrics-supplied software. This involved obtaining a master curve (horizontal and vertical shifts with 210°C as the reference temperature) and performing an Arrhenius fit of the shift factors.

RESULTS AND DISCUSSION

Mechanical Properties

The variation of flexural modulus and Charpy impact strength with HDPE content are shown in Figures 2 and 3. Data at 0% iPP are the values for pure HDPE. There is essentially no change in either property over the concentration range investigated, although there does appear to be a slight downward trend in flexural modulus and a slight upward trend in impact strength with increased HDPE content. This is in complete agreement with results published by Deanin and Sansone,[4] Teh,[5] Bartlett et al.,[6] and D'Orazio et al.[7] Teh observed a slight increase in impact strength for PP/LDPE blends, as did Bartlett et al. for PP/HDPE blends; and Deanin and Sansone and D'Orazio et al. observed a slight decrease in this property, also for PP/HDPE blends. There appears to be a slight conflict here. However, if one considers that the impact strength of the homopolymers are widely different in the present study (8 : 1 PE/PP) and in the case of Teh and Bartlett et al., but are similar in the study done by Deanin and Sansone and by D'Orazio et al., then the apparent contradiction disappears. In all cases, the experimental data lie below the straight line connecting the homopolymer impact strengths. Negative synergism is observed in all cases. In essence, then, our data serve to confirm the results of the authors mentioned above.

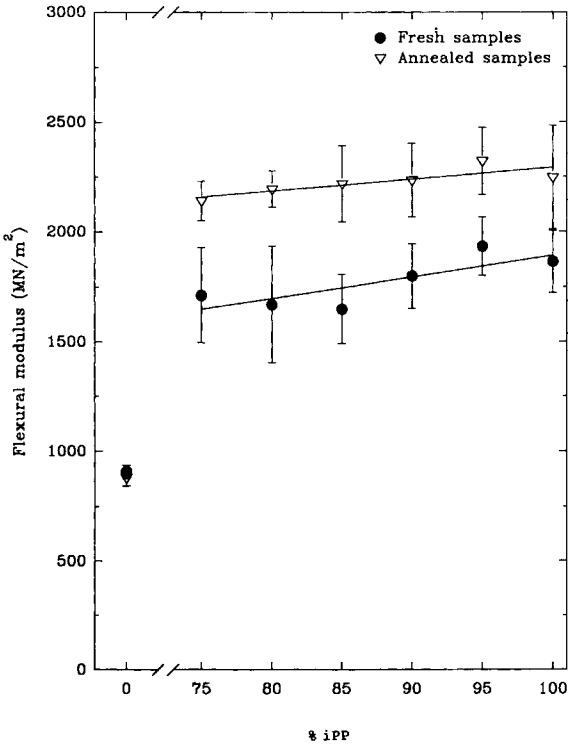

Figure 2 Effect of HDPE content on flexural modulus for fresh and annealed specimens of iPP, HDPE, and blends.

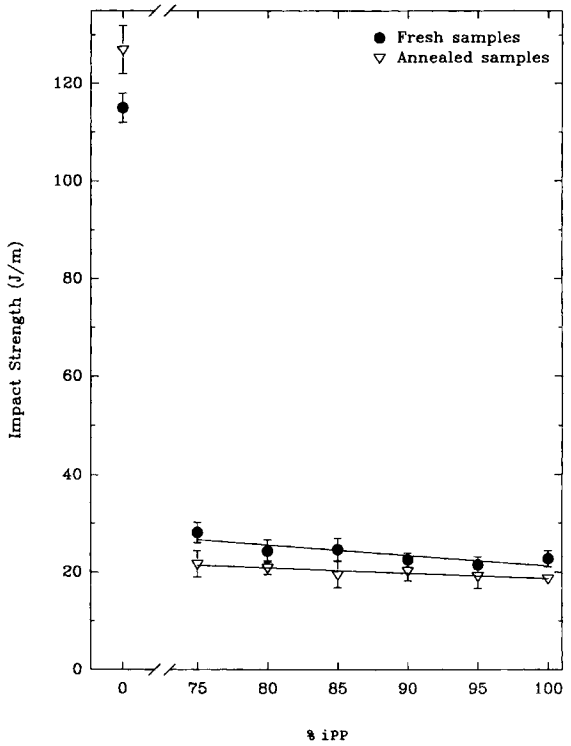

Figure 3 Effect of HDPE content on impact strength for fresh and annealed specimens of iPP, HDPE, and blends.

Figures 4–8 outline the variation of tensile properties with HDPE content in the iPP/HDPE blends. There was no observable change in the secant modulus (1.67% strain), nor in the yield stress (Figs. 4, 5). The yield strain (measured at the maximum yield stress) decreased slightly from about 8 to 7%, as shown in Figure 6. The tensile strength increased from 28 MPa for pure iPP to 32 MPa for the 80/20 blend. This is definitely a positive synergistic effect as the tensile strength of pure HDPE was 10 MPa.

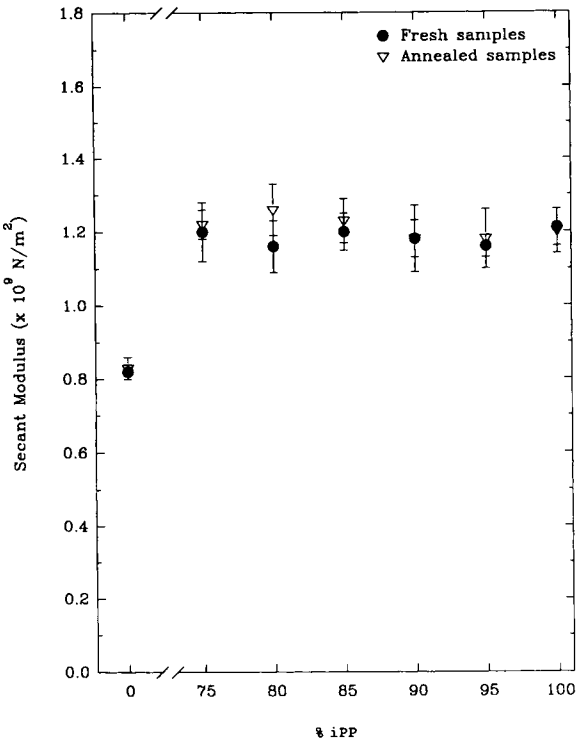

Figure 4 Effect of HDPE content on tensile secant modulus for fresh and annealed specimens of iPP, HDPE, and blends.

However, the elongation at break decreased with increasing HDPE content by about 50% compared to pure iPP. There does appear to be a maximum in the tensile strength at about 80% PP content, and a minimum in the yield strain and elongation at break at the same composition. This observation was not unexpected, however, because others have observed this previously in PP/PE blends. Our results are, in fact, generally consistent with the results of others[4-6,8-12] and confirm that iPP and HDPE are basically incompatible.

Because iPP and HDPE are incompatible, one should be concerned about the long-term service properties of PP that contained small amounts of HDPE. We have, therefore, exposed all samples to a 75°C condition for 7 days, and the effect of this treatment on the impact and the tensile properties is shown in Figures 2–8. The impact data suggest that the stiffness of the material has increased. The increase in the yield and the tensile strength and the decrease in elongation at break also indicate that annealing the samples resulted in a stiffer material, except that a corresponding increase in secant modulus was not observed. It is not clear at this time why we did not observe an increase in the secant modulus, because the flexural modulus showed a clear difference.

It is also apparent from these figures that the effect of annealing on any given sample is the same as on any other sample. In other words, the trends that were observed for the fresh samples as the HDPE content was varied are the same as the trends that were observed in the annealed samples.

Whereas the impact strength and the elongation at break of the blends decreased upon aging (Figs. 3, 8), the pure HDPE exhibited an increase in these properties. This observed reversal in effect of aging for pure HDPE is consistent with aging properties obtained for HDPE-rich PP/HDPE blends. This phenomenon will be discussed in a future article.

A number of phenomena have been postulated to account for the observed changes in the mechanical properties of polymer blends as they are aged. Because our samples were injection molded, we must consider internal stresses that were not able to relax because of the nonequilibrium conditions present during the injection molding. However, the relaxation of internal stresses that may occur as a result of annealing is difficult to gauge quantitatively.[13] Others have postulated that annealing at tempera-

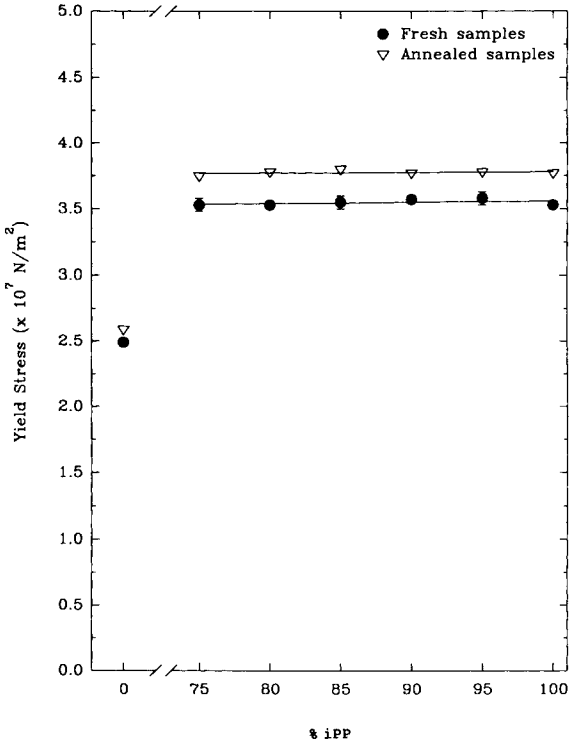

Figure 5 Effect of HDPE content on tensile yield stress for fresh and annealed specimens of iPP, HDPE, and blends.

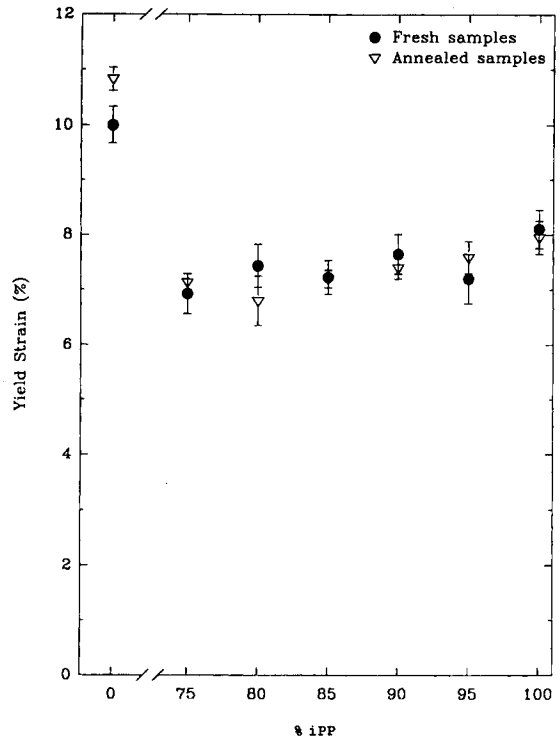

Figure 6 Effect of HDPE content on tensile yield strain for fresh and annealed specimens of iPP, HDPE, and blends.

tures between T_g and T_m results in secondary crystallization.[14,15] A material with a higher overall crystallinity would be stiffer and have a higher yield stress and tensile strength and a lower ultimate elongation, consistent with our results. There is, however, currently some controversy in this area. Yue and Msuya[16] recently studied the effect of physical aging (21°C in a cupboard) on the morphology of PP. They reported that aging of PP led to an increase in yield stress, which is consistent with our own results. They also determined from DSC analysis that aging had no apparent effect on the degree of crystallinity of the sample. However, they did observe a decrease in the activation volume of yielding as aging time increased. This was taken as an indication that little or no secondary crystallization took place, because an increase in crystallinity would have led to an increase in activation volume rather than the observed decrease. Their conclusion was that aging led to anything but secondary crystallization. Keijzers et al.[17] suggested that secondary crystallization in the case of PP led to the formation of new crystalites rather than to a perfectioning of the existing spherulites. In fact, they proposed that this secondary process involved the crystallization of the low molecular weight tail of the distribution. Our results indicate that aging at 75°C resulted in secondary crystallization, probably of both components of the blend, assuming that annealing had no effect on the relaxation of the internal stresses.

As far as the long-term, aged, properties of the iPP/HDPE blends are concerned, it will be clear that although the annealed materials have slightly inferior mechanical properties than the fresh materials, the change is not so significant as to render the blends useless. Annealing did not result in gross phase separation to produce a material devoid of any strength.

The impact and tensile data suggest that for the blends investigated, blending of iPP with HDPE resulted in a loss in ultimate elongation as more HDPE was added. However, we have seen that the impact strength was not greatly affected and the ultimate tensile strength was improved slightly. This indicates that one could injection mold parts that required an impact strength comparable to that of virgin iPP resin from a blend of iPP mixed with up to 10–15% HDPE. We deemed it prudent, nonetheless, to examine the properties of iPP/HDPE blends as they were manifested in a "real" part, namely, a thin-walled container,

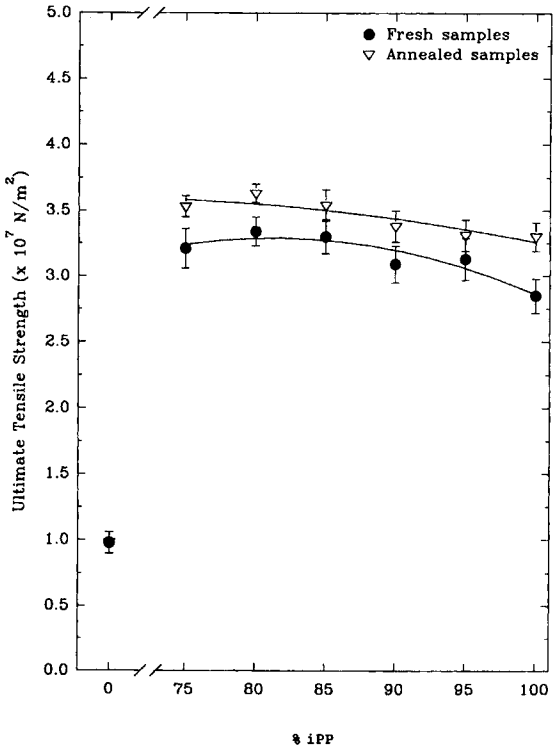

Figure 7 Effect of HDPE content on ultimate tensile strength for fresh and annealed specimens of iPP, HDPE, and blends.

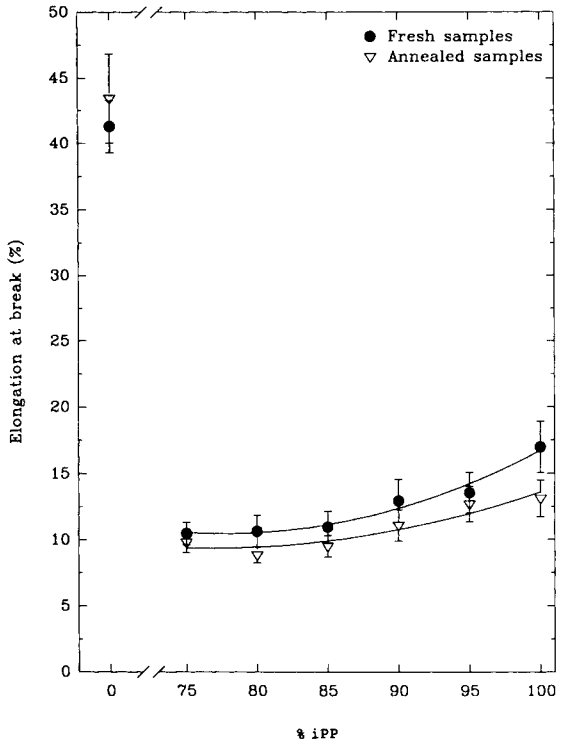

Figure 8 Effect of HDPE content on tensile elongation at break for fresh and annealed specimens of iPP, HDPE, and blends.

useful in applications such as dairy product tubs. The results of this study are presented in Figure 9. It is apparent from these test results that addition of a small amount of HDPE (5%) to iPP gave rise to a large drop in gate puncture strength. Addition of a further 5% HDPE caused the gate puncture strength to decrease to a level that is only 25% of the original, neat iPP, value. Further addition of HDPE had no effect. In all cases, failure occurred in a brittle mode. According to this test, therefore, mixing of iPP with a small amount of HDPE has a dramatic effect on the gate puncture strength. The results of annealing are also shown in Figure 9. The observation that the virgin iPP loses 75% of its strength as a result of annealing indicates either that the injection-molding conditions were far from optimal and the as-molded parts contained a great deal of internal stress around the gate region, or that the accelerated service test involved in annealing at 75°C for 1 week is unrealistically harsh for this product and application.

Thermal Properties

The results of our thermal (DSC) analysis of iPP/HDPE blends are summarized in Table III, and typical thermograms are shown in Figure 10. The melting onset temperature (not reported here) did not vary significantly with composition in any of the three experimental series. An examination of the heat of fusion data (which in our investigation can be considered to be a measure of the degree of crystallinity of the sample) suggests that there is an interaction between iPP and HDPE at some compositions. The variation of the corrected heat of fusion with composition for the quenched samples is shown in Figure 11. There are a number of important features to note in this figure. The first is that whereas the heat of fusion for the HDPE peaks varies greatly, there is only a small variation in the heat of fusion for the iPP peaks. This suggests that the iPP phase has a strong influence on the crystallization of the HDPE phase, and that the HDPE phase has only a small effect on the crystallization of the iPP phase. Of course, we must bear in mind that the iPP phase is the major component in these blends. The second feature to take notice of is that there is a pronounced maximum in the PE curve at a composition of 90/10 iPP/HDPE, and a corresponding slight minimum in the iPP curve at the same composition. The heat of fusion of PE for the 90/10 iPP/HDPE blend approaches the value of neat HDPE. This feature is

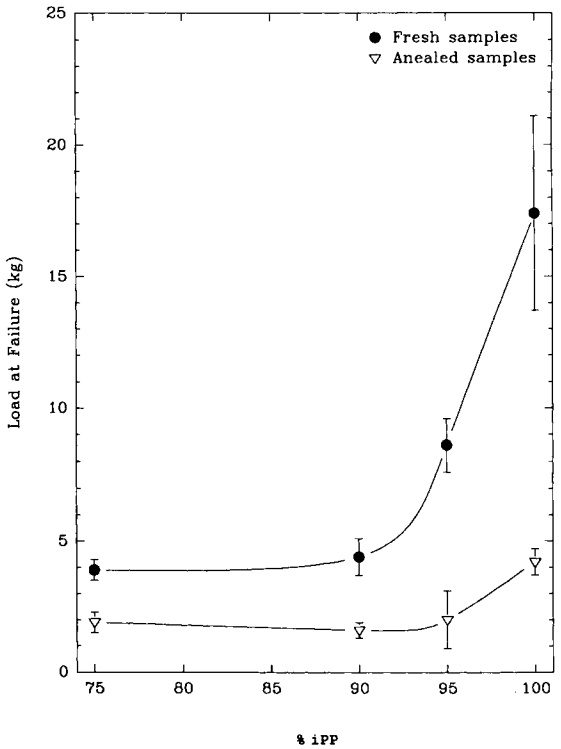

Figure 9 Effect of HDPE content on gate puncture load at failure for fresh and annealed specimens of iPP, HDPE, and blends.

Table III Summary of Thermal Analysis by DSC

	Heat of Fusion (J/g)		
	Melting[a]	Crystallization[b]	Remelting[c]
	HDPE Peaks		
% PE			
5	136.3	−134.6	183.5
10	142.3	−172.9	214.1
15	124.2	−147.9	173.7
20	115.7	−137.5	158.8
25	133.0	−157.3	168.4
100	145.3	−148.7	163.0
	PP Peaks		
% PP			
100	74.0	−76.8	86.7
95	73.7	−81.9	86.6
90	70.2	−76.9	79.3
85	71.0	−80.1	82.5
80	71.0	−81.1	81.4
75	66.1	−75.6	74.2

[a] 5°C/min heating rate.
[b] 1°C/min cooling rate.
[c] 5°C/min heating rate.

found also for the crystallization samples and for the slow-cooled samples. This observation suggests that the iPP phase has enhanced the degree of crystallinity of the HDPE phase, and that the HDPE phase has slightly reduced the overall crystallinity of the iPP phase at this composition. In other words, we have further evidence of an interaction between iPP and HDPE when the HDPE content is between 10 and 15%.

Table III also indicates that for the crystallization samples and for the remelted samples the heat of fusion of some of the blends was greater than the heat of fusion of the pure homopolymer. It is not clear why this is the case. It may be postulated that the crystallization kinetics or mechanism for the quenched and slow-cooled conditions are affected by the blending, possibly due to different interactions.

Lovinger and Williams,[9] in their investigation of PE/PP blends, observed a maximum in tensile modulus in blends containing ~ 80% PP. A detailed analysis of these blends by electron microscopy showed that addition of more than 10% PE to PP drastically reduced the spherulite size of the PP from ~ 100 to 5–10 μm. They suggested that this reduction in spherulite size resulted in a greater overall degree of crystallinity, and thus in a higher modulus at the synergistic composition of 80/20 PP/PE. They also observed intercrystalline links between PE domains by SEM. Both factors, the reduction in spherulite size and the existence of intercrystalline links, were thought to account for the increased tensile modulus.

It has been proposed by Bartczak et al.[18] that melt-blending of iPP and HDPE results in the migration of all heterogeneous nuclei from the iPP melt to the HDPE melt. The driving force was said to be interfacial free energy differences. Thus, in blends that were crystallized at temperatures above 127°C, the number of primary nuclei in the iPP was reduced, and the average spherulite size increased. In the case where crystallization took place below 127°C, the authors argued that two competing processes occurred. On the one hand, the PP melt was largely devoid of any heterogeneous nuclei. However, the presence of PE crystallites at the PP/PE interface provided heterogeneous nuclei for the PP. And because the original heterogeneous nuclei had migrated from the PP phase to the PE phase, there were a great number of PE crystallites that could act as nuclei for the PP. The net result was an increase in the number of PP spherulites and, consequently, a decrease in the average size of the spherulites.

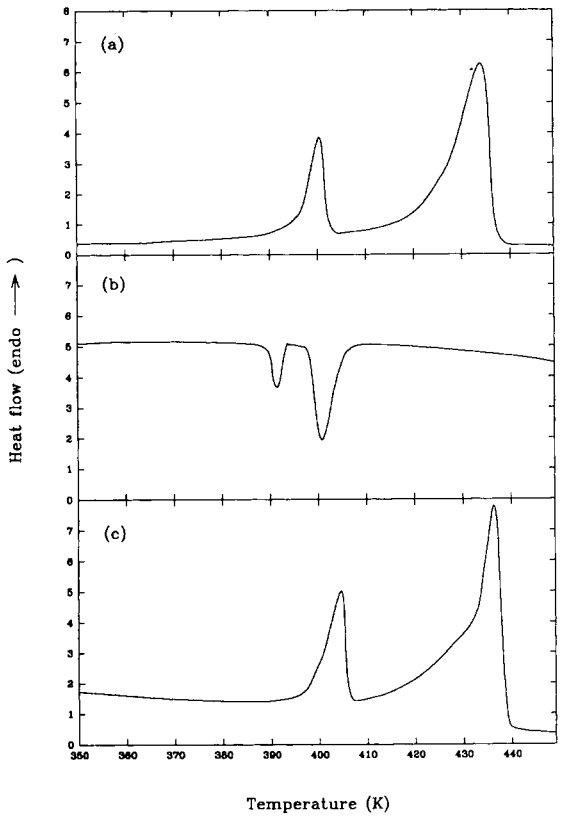

Figure 10 Typical thermograms obtained for the iPP/HDPE blends. (a) Melting endotherm of quenched sample. (b) Crystallization exotherm of melted sample. (c) Melting endotherm of slow-cooled sample. All data are for the 90/10 PP/HDPE blend.

We recently reported[19] on the application of dynamic mechanical methods to the study of the crystallization behavior of PP and PP/HDPE blends. Isothermal crystallization at 136°C was studied by dynamic mechanical analysis and hot-stage optical microscopy. It was shown that the overall nucleation density passed through a minimum at an HDPE content of 10–15%. Under constant-cooling-rate conditions, it was found that the nucleation and crystallization processes for PP could be distinguished by dynamic mechanical analysis. Under a cooling rate of 1°C/min, nucleation was seen to begin at about 150°C, while crystallization was not observed until about 130°C. This was not observed for HDPE. Instead, a rapid increase in modulus occurred at about 125°C, which was attributed to instantaneous nucleation followed immediately by crystallization of the HDPE. Addition of even a small amount of HDPE (5%) to PP resulted in HDPE-like behavior, with both the PP and the HDPE crystallizing at the same time, with no observable nucleation region. The nucleation and crystallization onset temperature was found to vary with HDPE content. Interestingly, addition of 10% HDPE resulted in the largest change in the crystallization onset temperature. This blend (90/10 PP/HDPE) behaved almost like pure HDPE under 1°C/min crystallization conditions. It would seem from these results that the crystallization behavior of the HDPE is affected, which is consistent with the results that were obtained by thermal analysis in this present study.

Dynamic Mechanical Properties

The variation of complex viscosity (η^*) with frequency (ω) at 180°C for all the blends and for both of the homopolymers is shown in Figure 12. A typical master curve for the 90/10 iPP/HDPE blend is shown in Figure 13. It is clear that we are not observing simple behavior. First, the curves for the homopolymers exhibit a crossover point at a frequency of about 1 rad/s. We would expect that for a "well-behaved" system the viscosities of the blends would lie between the curves for the homopolymers. This is closely followed by blends of low HDPE contents. However, this is not true in the case of 85/15, 80/20, and 75/25 blends. The 75/

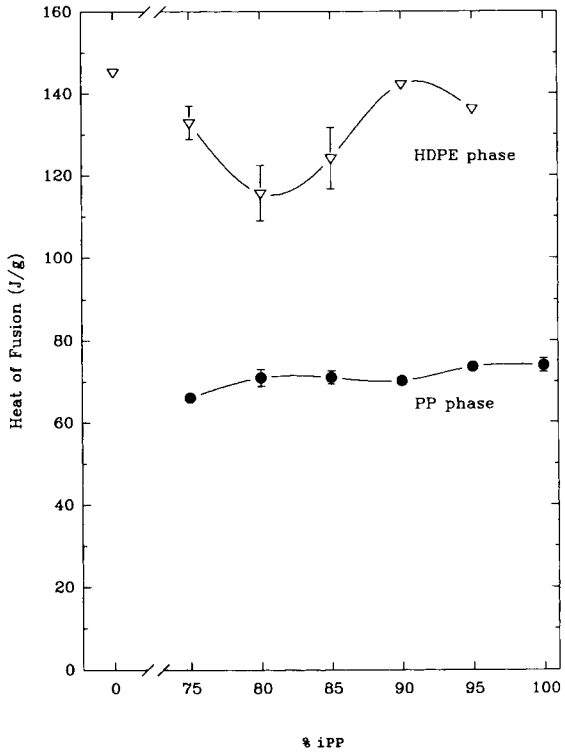

Figure 11 Variation of heat of fusion of PP and HDPE with HDPE content.

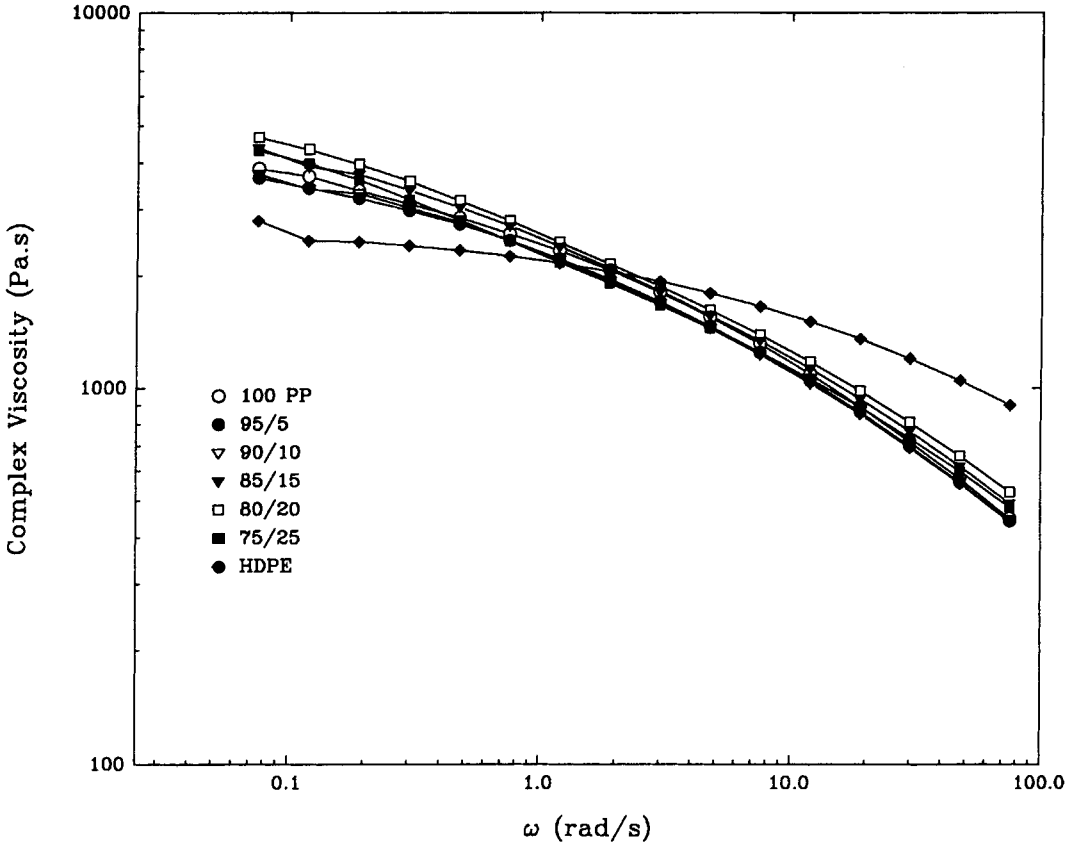

Figure 12 Variation of complex viscosity with frequency for all the blends at 180°C.

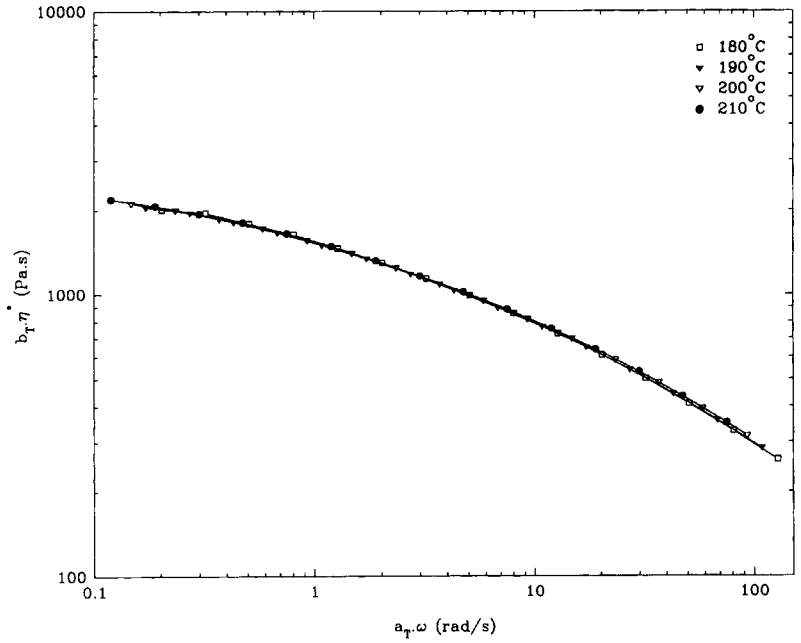

Figure 13 Master curve for the η^* vs. ω data for the 90/10 iPP/HDPE blend by horizontal and vertical shift of flow curves at four temperatures.

25 blend, for instance, exhibits a complex viscosity outside the range defined by the homopolymers at low shear rates, but lies within the range at high shear rates.

The effect of adding HDPE to PP is shown more clearly from the zero shear viscosity plot in Figure 14. Addition of a small amount of HDPE to iPP has a greater effect at higher temperatures. Because the zero shear viscosity of the HDPE is lower than those of PP and the blends, a peak can be inferred for the 20–25% HDPE at 180°C. It also appears that the composition at which a peak in η_o occurs moves toward the high PE end with increasing temperature. This latter observation may be due to the fact that the ratio η_o(PP) : η_o(HDPE) decreases with temperature, as shown in Figure 15. These data suggest that the observations on the solid-state properties that inferred interactions at certain compositions are also observed in the melt state. This becomes even more apparent when we look at the variation of activation energy for flow with composition (Fig. 16). Clearly, there exist some interactions in the molten state at a composition of 90/10 that results in a maximum in the activation energy. The exact nature of this interaction is not clear to us and further investigation is required.

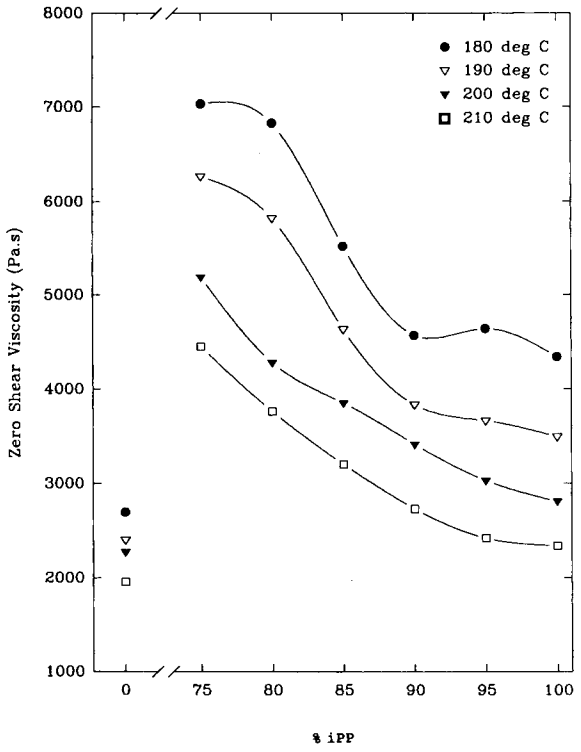

Figure 14 Effect of HDPE content on the zero-shear viscosity, at 180°, 190°, 200°, and 210°C.

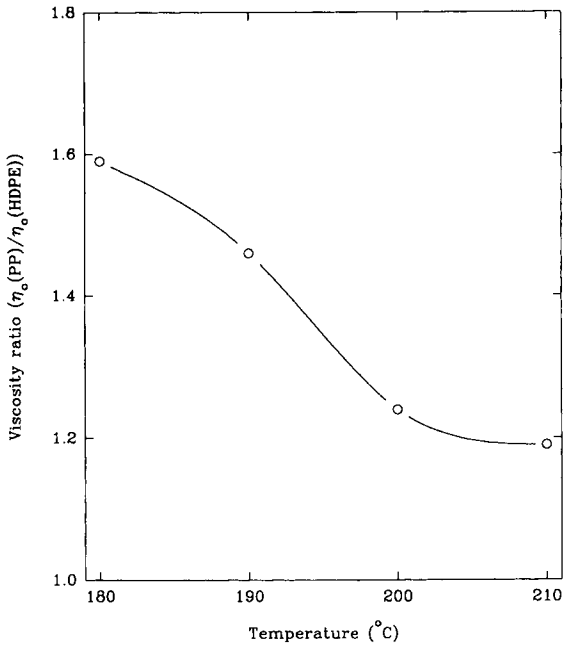

Figure 15 Variation of η_o(PP) : η_o(HDPE) with temperature.

CONCLUSIONS

Our investigation into the physical, thermal, and rheological properties of PP/HDPE blends allows us to make the following conclusions and general observations.

1. Based on the physical properties of these blends (especially the yield behavior and the ultimate elongation in tensile deformation), it is clear that iPP and HDPE are basically incompatible and immiscible at the concentrations studied.
2. When considering this incompatibility and immiscibility, one must be concerned about the long-term stability and performance of iPP/HDPE blends. It has been shown that aging of injection-molded specimens from these blends caused a slight decrease in tensile and impact properties, but the net effect is not serious, except for the impact strength of the gate region in the high-shear-flow thin-wall sections.
3. The evidence that indicates a special interaction at an HDPE content of 10–20% continues to grow. We have observed evidence for this interaction in tensile properties, thermal properties, melt flow properties, and crystallization behavior.

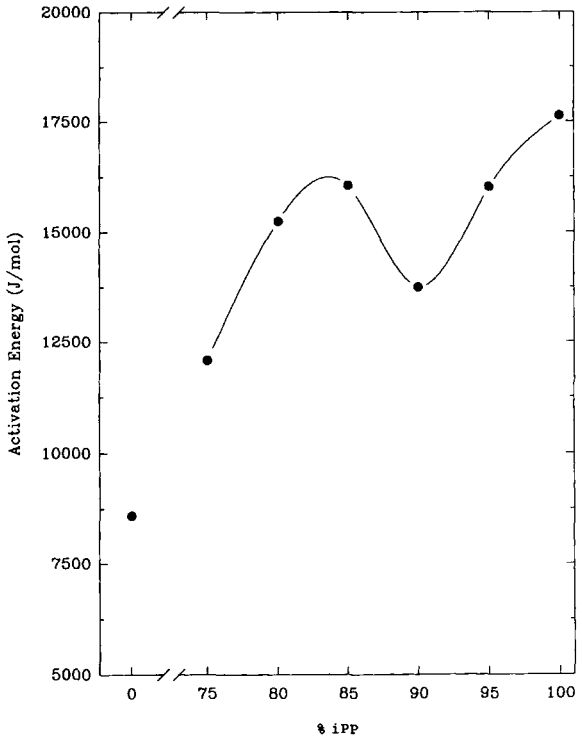

Figure 16 Effect of HDPE content on activation energy for flow of iPP, HDPE, and blends.

The authors thank the Natural Sciences and Engineering Research Council of Canada, the University Research Incentive Fund of Ontario, and Shell Canada Limited for financial support. Thanks also to G. Shields of Shell Canada for assistance with the gate puncture testing.

REFERENCES

1. S. Pang and A. Rudin, in *ACS Symposium Series 521, Chromatography of Polymers: Characterization by SEC and FFF*, Th. Provder, Ed., American Chemical Society, Washington, D.C., 1993.
2. D. G. Cook, A. Rudin, and A. Plumtree, *Polym. Eng. Sci.*, **30,** 596 (1990).
3. Z. Tadmor and C. G. Gogos, *Principles of Polymer Processing*, Wiley, New York, 1979.
4. R. D. Deanin and M. F. Sansone, *Polym. Prepr.*, **19,** 211 (1978).
5. J. W. Teh, *J. Appl. Polym. Sci.*, **28,** 605 (1983).
6. D. W. Bartlett, J. W. Barlow, and D. R. Paul, *J. Appl. Polym. Sci.*, **27,** 2351 (1982).
7. L. D'Orazio, R. Greco, C. Mancarella, E. Martuscelli, G. Ragosta, and C. Silvestre, *Polym. Eng. Sci.*, **22,** 536 (1982).
8. O. F. Noel, III and J. F. Carley, *Polym. Eng. Sci.*, **15,** 117 (1975).
9. A. J. Lovinger and M. L. Williams, *J. Appl. Polym. Sci.*, **25,** 1703 (1980).
10. A. K. Gupta, V. B. Gupta, R. H. Peters, W. G. Harland, and J. P. Berry, *J. Appl. Polym. Sci.*, **27,** 4669 (1982).
11. A. K. Gupta and S. N. Purwar, *J. Appl. Polym. Sci.*, **30,** 1799 (1985).
12. R. A. Varin and D. Djokovic, *Polym. Eng. Sci.*, **28,** 1477 (1988).
13. J. R. White, *J. Mater. Sci.*, **20,** 2377 (1985).
14. A. Sharples, *Introduction to Polymer Crystallization*, Edward Arnold (Publishers) Ltd., London, 1966.
15. M. Dosière, Ed., *Crystallization of Polymers*, Kluwer Academic Publishers, Dordrecht, 1993.
16. C. Y. Yue and W. F. Msuya, *J. Mater. Sci. Lett.*, **9,** 985 (1990).
17. A. E. M. Keijzers, J. J. van Aartsen, and W. Prins, *J. Am. Chem. Soc.*, **90,** 3107 (1968).
18. Z. Bartczak, A. Galeski, and M. Pracella, *Polymer*, **27,** 537 (1986).
19. J. W. Teh, H. P. Blom, and A. Rudin, *Polymer*, **35,** 1680 (1994).

Received March 3, 1995
Accepted April 19, 1995